

# AD730™ - A NEW NICKEL-BASED SUPERALLOY FOR HIGH TEMPERATURE ENGINE ROTATIVE PARTS

A. Devaux<sup>1</sup>, B. Picqué<sup>2</sup>, M.F. Gervais<sup>1</sup>, E. Georges<sup>1</sup>, T. Poulain<sup>1</sup>, P. Héritier<sup>3</sup>

<sup>1</sup> Aubert & Duval, Site des Ancizes BP1, 63770 Les Ancizes Cedex, France

<sup>2</sup> Aubert & Duval, 75 boulevard de la Libération, BP 173, 09102 Pamiers Cedex, France

<sup>3</sup> Aubert & Duval, Parc Technologique La Pardieu, 6 rue Condorcet, 63063 Clermont-Ferrand Cedex 1, France

Keywords: AD730™, cast and wrought, disk, creep, tensile, solution heat treatment, cooling rate, microstructural stability

## Abstract

The enhancement of efficiency in gas turbine engines requires the development of new superalloys capable of withstanding higher temperatures. The development of new industrial cast and wrought (C&W) disk alloys with required combination of strength, creep and fatigue properties at 700°C is highly desired due to the expensive cost of powder metallurgy. AD730™, which is the newly nickel base superalloys developed by Aubert & Duval, was therefore designed to offer a better combination between high temperature properties at 700°C and cost compared to other C&W superalloys. This paper describes the alloy design based upon the chemistries of the previous experimental alloys Ni30 and Ni33 [1-2]. The control of expensive elements contents and the presence of iron in AD730™ alloy confer to this alloy an attractive cost compared to other C&W superalloys for disk applications. Gamma prime solvus was decreased compared to Ni33 in order to improve hot workability and (Ti+Nb)/Al ratio was decreased compared to Ni30 and Ni33 in order to avoid any risk of Eta-phase precipitation. It was actually observed that the precipitation of the needle-shape Eta-phase predicted by the thermodynamic databases was not in agreement with experimental results obtained on various alloys of the AD730™ chemical system. Industrial ingots with a diameter equal to 500mm were produced (Vacuum melting and remelting) and converted to evaluate the mechanical properties and the ability for the conventional C&W route. A special attention is made in this paper to the AD730™ workability which was highly evaluated with various industrial forging process routes (close-die forging, ring-rolling...etc). Heat treatment optimization was then performed on this alloy in regard to tensile and creep properties. The effect of solution heat-treatment temperature and cooling rate after solution heat treatment were investigated on AD730™. Solution heat treatment temperature has a slight effect on the tensile strength if the temperature is lower than the gamma prime solvus. Yield strength remains stable and close to 1100MPa at 700°C. Solution heat-treatment was therefore optimized in regard of grain size in order to increase creep properties. As most of superalloys strengthened by gamma prime phase, cooling rate after solution heat-treatment has to be as fast as possible to get the highest tensile and creep properties.

Oil quenching can be easily performed on AD730™ without any issues due to the moderate gamma prime content in the alloy (35-40%) and the fine grain size. Tensile, creep, long-term aging performed on a forged disk heat-treated in optimized conditions, are presented and discussed in this paper. A comparison with Udimet720™ properties and 718Plus™ ones show that AD730™ alloy presents a higher combination between cost and mechanical properties at 700°C than current C&W superalloys.

## Introduction

The latest design of high-efficiency engines has high requirements for the mechanical properties and temperature capability of the key components, especially the stages of disk where the stress and temperature are the highest. Alloy development for turbine disk with high properties up to 700°C is consequently crucial in order to improve the thermal efficiency in gas turbine engines. 718 superalloy is extensively used for turbine disk due to its moderate cost. However, this superalloy is not capable of withstanding temperatures higher than 650°C due to the coarsening of the strengthening phase gamma double prime above this temperature [3-5]. New  $\gamma/\gamma'$  superalloys (René88DT, N18, RR1000...etc) were therefore developed to withstand higher temperature on the turbine discs. These superalloys can not be processed by the conventional cast & wrought (C&W) route due to their high  $\gamma'$  fraction and require therefore a processing by the expensive powder metallurgy route. Progress was made on C&W route, especially with the development of triple melt which allowed the manufacturing of alloys such U720Li™, Waspaloy™, and more recently TMW4 and 718Plus™. These superalloys present various combinations between cost and mechanical properties. However it can be considered that 718Plus and TMW4 do not improve the combination between cost and mechanical properties currently offered by U720Li. TMW4 shows higher properties than U720Li [6-8] but is significantly more expensive due to its high cobalt content. Inversely, 718Plus [9-10] presents a lower cost (presence of iron and reasonable cobalt content) but restricted creep properties at 700°C compared to the current U720Li disk alloy.

	Ni	Fe	Co	Cr	Mo	W	Al	Ti	Nb	B	C	Zr	P
<b>718</b>	Base	18	-	18	3	-	0.5	1	5.4	0.004	0.03	-	0.01
<b>718Plus</b>	Base	10	9	18	2.75	1	1.5	0.7	5.5	0.004	0.02	-	0.01
<b>Waspaloy</b>	Base	-	13.5	19.5	4.25	-	1.5	3	-	0.006	0.05	0.03	-
<b>U720Li</b>	Base	-	15	16	3	1.25	2.5	5	-	0.015	0.015	0.03	-

Table 1: Chemical analysis of various C&W disk superalloys

The new nickel base AD730<sup>TM</sup> superalloy developed by Aubert & Duval was designed to improve the combination between high temperature properties and cost of the current C&W disk superalloys with these following features:

- mechanical properties close to U720Li and significantly higher than 718Plus, Waspaloy and 718
- cost equal to 718Plus and lower than U720Li and other  $\gamma/\gamma'$  superalloys for turbine discs

This paper describes the design of AD730<sup>TM</sup> and the results obtained on full scale production.

### Design of AD730

The design of AD730<sup>TM</sup> was based upon results obtained on Ni30 and Ni33 alloys. As Ni30 and Ni33 presented high mechanical properties up to 700°C and a moderate cost compared than other  $\gamma/\gamma'$  superalloys [2], these alloys were selected for the final design. All the criteria defined for the design of Ni30 and Ni33 [1] were kept to adjust the final chemistry. Only slight modifications were made to Ni30 and Ni33 in order to improve their workability and their microstructural stability in regard of  $\eta$ -Eta phase precipitation. As shown in table 2, the chemistry of AD730<sup>TM</sup> is actually quite similar to those of Ni30 and Ni33. The presence of iron and the control of expensive elements provide to AD730<sup>TM</sup> a lower cost than other C&W superalloys (figure 1). The (Ti+Nb)/Al ratio was supposed to be in relation with  $\gamma/\gamma'$  mismatch and to have a strong effect on hot mechanical properties. It was the reason why high ratio values were selected during alloy design of Ni30 and Ni33. These ratio values were nevertheless restricted by the precipitation of deleterious  $\eta$ -Eta phase which was predicted by Thermo-Calc to appear for ratio larger than 3 as shown on figure 2. However,  $\eta$ -Eta phase was experimentally observed in Ni50 and Ni40 which respectively have (Ti+Nb)/Al ratio values equal to 2.5 and 3. These results show that the precipitation of  $\eta$ -Eta phase is not accurately predicted in this chemical system but also that (Ti+Nb)/Al ratio values of Ni30 and Ni33 were too high to fully avoid  $\eta$ -Eta phase precipitation even if this phase was not observed in both alloys. A (Ti+Nb)/Al ratio close to 2 was therefore selected for the final composition assuming that only a slight effect should be observed on mechanical properties due to the decrease of this ratio [11]. It is the reason why tungsten content was slightly increased in AD730<sup>TM</sup> in order to counterbalance the potential effect of the decrease of (Ti+Nb)/Al ratio on the mechanical properties. Secondly, a special attention was paid to the workability of the final alloy. A good workability above and below  $\gamma'$  solvus was researched to easily control the microstructure on billets and to promote a convenient ingot conversion process. Upsetting tests were performed on Ni30, Ni33 and U720 at 1160°C with a strain equal to 0.85 and a transfer time equal to 30 seconds. No coatings were used to provide a thermal protection to the sample.

Consequently, a decrease of temperature was observed on the surface of the sample before upsetting and has lead to the appearance of cracks for the alloys with the higher  $\gamma'$  contents. As shown on figure 3, the higher the  $\gamma'$  solvus, the lower the workability due to the precipitation of  $\gamma'$  phase during cooling which starts for these alloy at a temperature close to solvus  $\gamma'$  minus 30-35°C. A  $\gamma'$  solvus close to 1100°C was therefore researched for the final composition to guaranty a good workability over a large temperature range. These new criteria, added to the initial ones [1], explain the increase of Al content compared to Ni30 and the decrease of Ti and Nb contents compared to Ni33. The  $\gamma'$  fraction of AD730<sup>TM</sup> at 700°C was estimated by Thermo-Calc to be close to 37% and is intermediate between those of Ni30 (35%) and Ni33 (39%) [1].

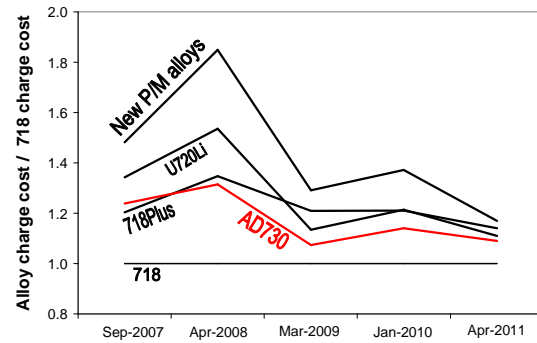


Figure 1: C&W superalloys costs calculated with raw material content (costs rationalized to 718's) over a period of 4 years

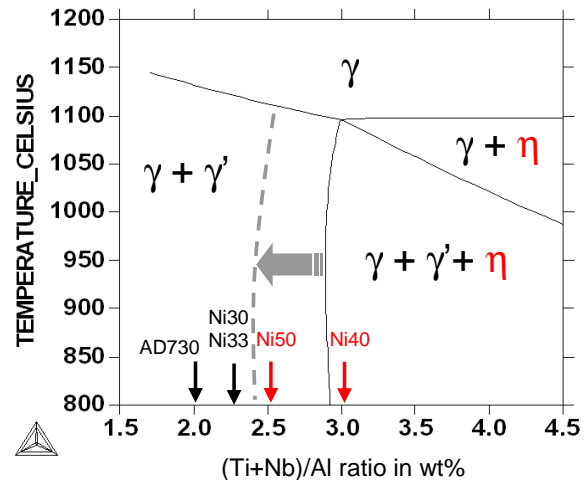


Figure 2:  $\eta$  phase stability in function of temperature and (Ti+Nb)/Al wt% ratio values according Thermo-Calc software for compositions in table 2.

	Ni	Fe	Co	Cr	Mo	W	Al	Ti	Nb	B	C	Zr	(Ti+Nb)/Al wt%	Presence of $\eta$ -Eta
Ni30	Base	5	9	15.2	3	2.5	2.0	3.5	1	0.01	0.015	0.03	2.25	No
Ni50	Base	5.6	9.5	15.2	3	2.5	2.0	3.8	1.2	0.01	0.015	0.03	2.5	Yes +
Ni40	Base	5	9	15.3	3	2.5	1.75	3.9	1.3	0.01	0.01	0.03	3	Yes ++
Ni33	Base	3.2	9.2	14.8	2.9	2.3	2.3	4	1.3	0.01	0.015	0.03	2.3	No
AD730 <sup>TM</sup>	Base	4	8.5	15.7	3.1	2.7	2.25	3.4	1.1	0.01	0.015	0.03	2	No

Table 2 : Chemical analysis of AD730<sup>TM</sup> alloy compared to other C&W disk superalloys

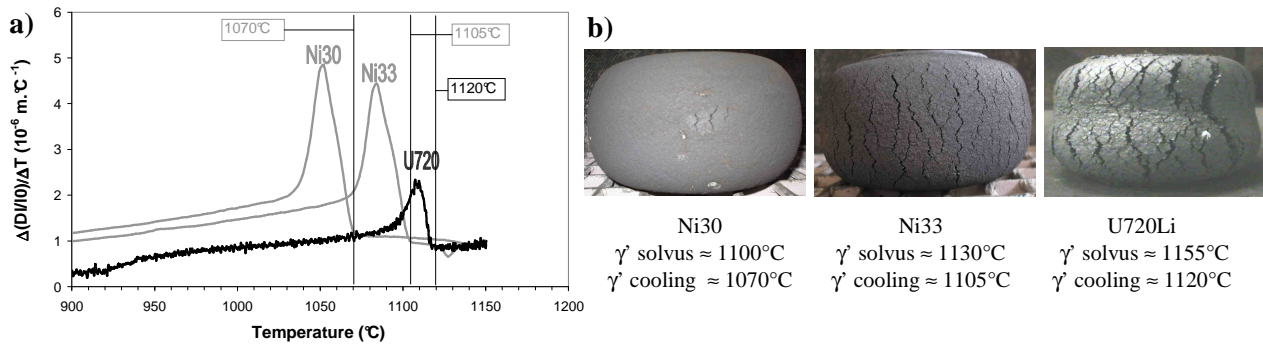


Figure 3: Correlation between  $\gamma'$  starting precipitation temperature during cooling ( $\gamma'$  cooling) and workability. a) Derivative cooling curves of dilatometric tests performed from 1160°C with a cooling rate equal to 5°C/min. b) Upsetting tests performed at 1160°C with a strain equal to 0.85 and a transfer time of 30 seconds (no coating).

### Experimental procedure

A first ten tons VIM heat was melted in AD730<sup>TM</sup>. One ingot with a diameter equal to 500mm was vacuum arc remelted and then converted to obtain a billet with a diameter equal to 200mm. The conversion was made with a 4500 tons press and a rotative forging machine above and below  $\gamma'$  solvus. These billets did not present any cracks and any defects. These billets were used to forge full scale disk trials with various forging processes. Close-die forged and ring-rolled discs with an external diameter close to 600mm (figure 4) were forged below  $\gamma'$  solvus in the 1050°C-1090°C temperature range. As shown on figure 5, microstructure was observed at different steps of the manufacturing process. As expected,  $\eta$ -Eta phase was only observed on VAR ingot in the interdendritical spaces where the Nb and Ti contents were the highest and was easily removed with a homogenization performed in the 1160°C-1220°C temperature range. The ingot conversion process leads to a grain size on the billet close to ASTM 8 ALA 6. The grain size on forged discs was significantly finer and close to ASTM 12. Primary  $\gamma'$  precipitates appeared at grain boundaries during subsolvus forging and were therefore observed on billets and discs. The primary  $\gamma'$  distribution was more homogeneous on discs and is strongly linked with the amount of strain below  $\gamma'$  solvus. The effect of solution heat treatment temperature and cooling rate after solution heat treatment were studied on billet with tensile and creep tests. Mechanical tests were then performed on discs heat-treated in the optimized conditions previously defined on billets.

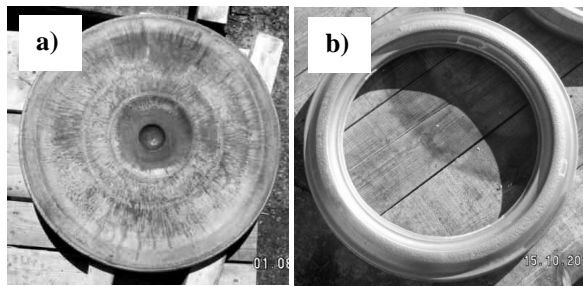


Figure 4 : Close-die forged disk (a) and ring-rolled + close-die forged disk (b) with external diameter of 600mm

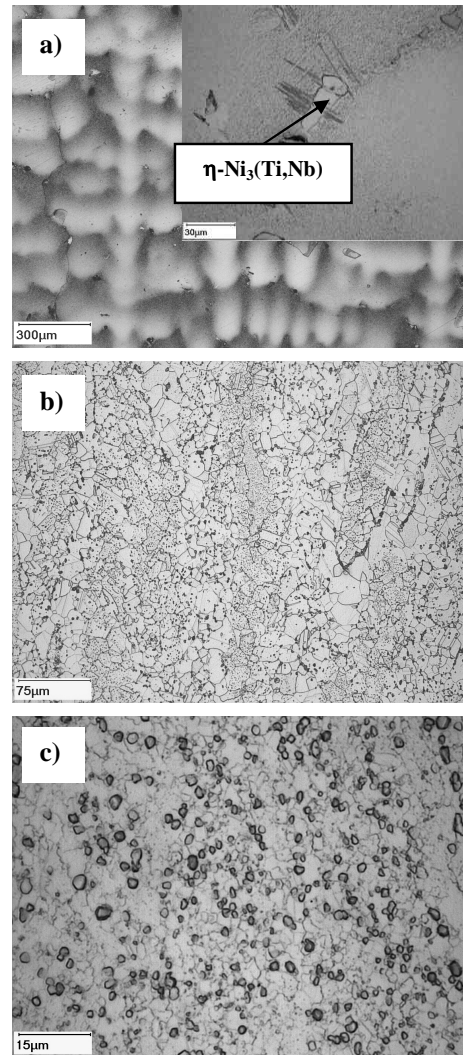


Figure 5 : AD730<sup>TM</sup> microstructure observed on a) VAR ingot b) 200mm diameter billet b) close-die forged disk

### Workability of AD730™

Workability was evaluated at various steps of the process with preliminary laboratory tests and industrial tests in a second time. Workability of AD730™ was assessed in laboratory with tensile tests performed at high temperature and high strain rate. First tests were performed with samples taken into a slice of VAR ingot in order to check the workability before ingot conversion. These tests were performed after homogenization with a strain rate equal to  $10^{-1} \text{ s}^{-1}$  in the 1040°C-1220°C temperature range. As shown on figure 6, a comparison was established with U720Li and Waspaloy alloys tested in similar conditions in terms of strain rate and initial state (homogenized ingot). AD730™ workability evaluated on ingot is higher than those of U720Li and Waspaloy which can not be respectively forged in these conditions above and below  $\gamma'$  solvus contrary to AD730™. It is the reason why the grain size on Waspaloy billets is not very fine (conversion made at high temperature) and the forging process of U720Li billet is difficult (conversion made at low temperature). The ability to be forged either below or above  $\gamma'$  solvus confers to AD730™ the opportunity to break the as-cast structure at high temperature above  $\gamma'$  solvus and to refine the microstructure by a reasonable amount of strain below  $\gamma'$  solvus with a convenient forging process.

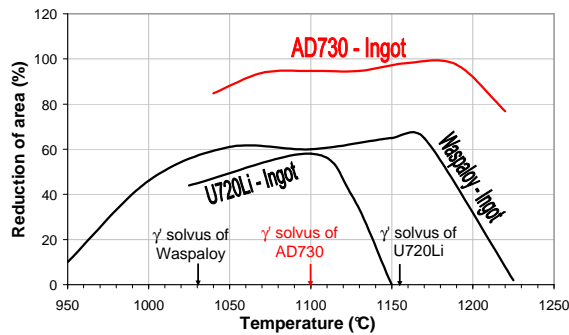


Figure 6 : Reduction of areas measured with tensile tests on ingot at different temperatures for various superalloys

Same tests were performed on billets with a finer microstructure and at lower temperatures. In the same way, a comparison was made with other C&W disk superalloys (figure 7).

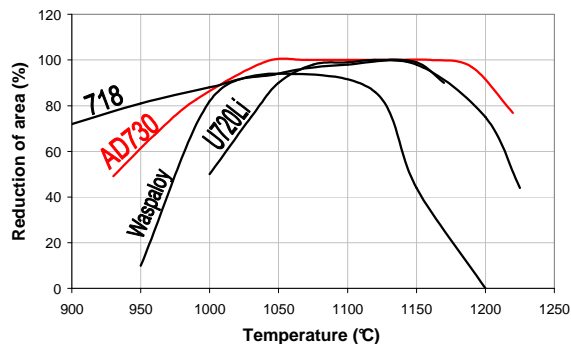


Figure 7 : Reduction of areas measured with tensile tests on forged billet at different temperatures for various superalloys

These tests show that the workability on billets of AD730™ is between those of 718 and Waspaloy. These tests indicate actually that cracking is respectively possible on Waspaloy and AD730 below 980°C and 930°C. The behavior of AD730™ in terms of cracking sensitivity was evaluated to be intermediate between those of 718 and Waspaloy. These laboratory results were confirmed in industrial conditions with ring-rolling and close-die forging tests. As shown on figure 8, no cracks were observed during the manufacturing process of the discs presented on figure 4. The results confirm the good ability of AD730™ for the conventional C&W route.

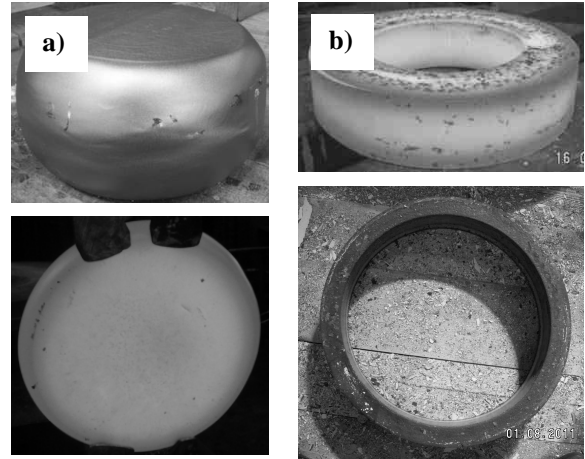


Figure 8: Intermediate steps to obtained discs with external diameter of 600mm on figure 4. Open die forging operations (a) and ring-rolling operations (b) before close die forging

### Effect of solution heat treatment

The solution heat-treatment temperature was studied on small blanks with a section of 16x16 mm<sup>2</sup> taken at mid-radius of the 200mm diameter billet. These blanks were solution heat-treated at 1060°C, 1070°C, 1080°C and 1120°C during four hours before being cooled in air. Air cooling on these blanks leads to a cooling rate close to  $200^{\circ}\text{C} \cdot \text{min}^{-1}$  and approximates the cooling rate of oil quenched disks. The samples were then aged at 760°C during 16h. Tensile tests at 700°C and creep tests at 750°C under a stress of 450MPa were performed to evaluate the effect of solution heat treatment temperature (table 3). In the same way, cooling rate after solution heat treatment was studied with various cooling rates performed after a solution heat-treatment of four hours at 1080°C. Tensile tests at 700°C and creep tests at 700°C under a stress of 690MPa were performed to evaluate the effect of this parameter (table 4). No effect of solution heat treatment temperature on grain size was observed except for the temperature of 1120°C which is above the  $\gamma'$  solvus and logically leads to a larger grain size. Solution heat treatment temperature has a slight effect on the tensile strength if the temperature is lower than the gamma prime solvus (figure 9). Yield strength remains actually stable and close to 1100MPa at 700°C. A supersolvus solution heat-treatment does not have any effect on UTS but rather on yield strength. The solution heat treatment temperature has a strong effect on creep life even if the solution heat-treatment temperature is below  $\gamma'$  solvus and the grain size almost the same (figure 10).

A decrease of elongation for tensile and creep tests is observed for the supersolvus heat-treatment: this is probably due to the larger grain size and the absence of primary  $\gamma'$  precipitates at grain boundaries (figure 11).

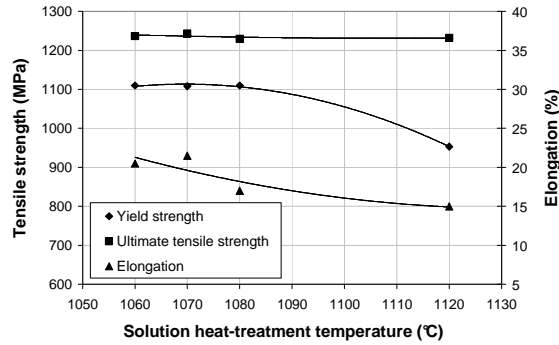


Figure 9: Effect of solution heat treatment temperature on tensile properties at 700°C

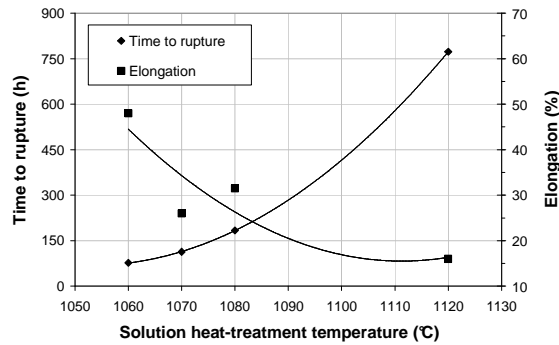


Figure 10: Effect of solution heat treatment temperature on creep properties at 750°C-450MPa

As expected, cooling rate after solution heat-treatment has a strong effect on tensile and creep properties. A high cooling rate after solution heat-treatment promotes higher tensile strength and higher creep lives (figure 12-13). Inversely, high cooling rates decrease elongation for tensile and creep tests. SEM-FEG examinations were also performed to analyze the effect of solution heat treatment temperature and cooling rate on  $\gamma'$  precipitation inside the grains (Figure 14). The sizes of secondary  $\gamma'$  precipitates that have precipitated during cooling after solution heat-treatment were measured and are indicated in tables 3 and 4. An increase of solution heat-treatment temperature leads to larger secondary  $\gamma'$  precipitates in relation with a precipitation during cooling which occurs at a higher temperature. A similar tendency was observed in U720Li [12] and can be easily checked with dilatometric tests.

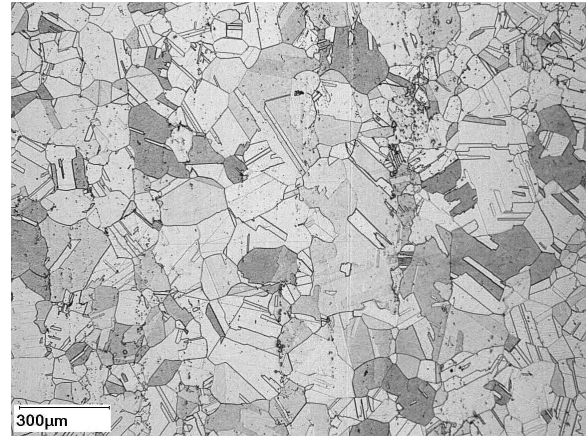


Figure 11: microstructure and grain size obtained after supersolvus heat treatment 1120°C/4h/200°C/min

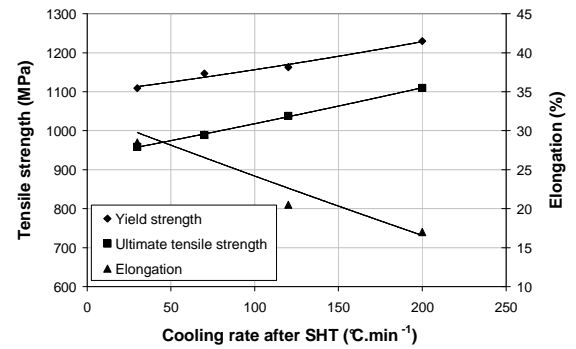


Figure 12: Effect of cooling rate after solution heat-treatment on tensile properties at 700°C

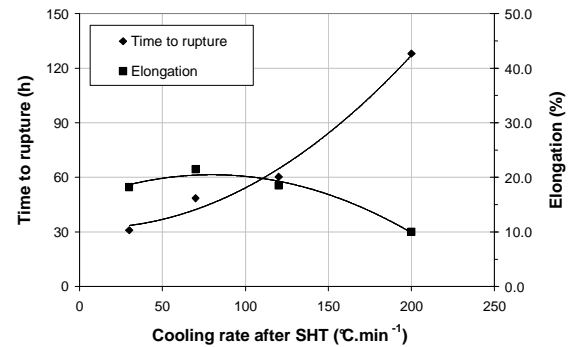


Figure 13: Effect of cooling rate after solution heat-treatment on creep properties at 700°C-690MPa.

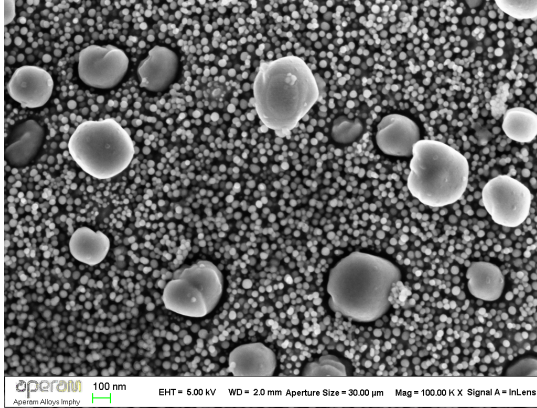
Solution heat treatment	Aging	Grain size ASTM	Secondary $\gamma'$ diameter (nm)	Tensile test at 700°C				Creep 750°C/450MPa		
				UTS (MPa)	YS (MPa)	El (%)	RA (%)	Rupture time (h)	El (%)	RA (%)
1060°C/4h/200°C/min	760°C/16h	8.5	40nm - 270nm	1237	1110	20.5	19	77	48	64
1070°C/4h/200°C/min	760°C/16h	8.5	Not determined	1243	1108	21.5	20	113	26	60
1080°C/4h/200°C/min	760°C/16h	8	50nm	1230	1110	17	18	184	32	43
1120°C/4h/200°C/min	760°C/16h	3	60nm	1232	953	15	17	773	16	18

Table 3 : effect of solution heat-treatment temperature on mechanical properties and microstructure

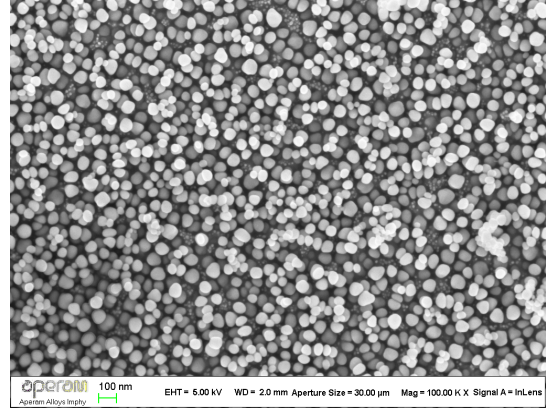


Solution heat treatment	Aging	Grain size ASTM	Secondary $\gamma'$ diameter (nm)	Tensile test at 700°C				Creep 700°C/690MPa		
				UTS (MPa)	YS (MPa)	El (%)	RA (%)	Rupture time (h)	El (%)	RA (%)
1080°C/4h/200°C/min	760°C/16h	8.5	50nm	1230	1110	17	18	128	10	26
1080°C/4h/120°C/min	760°C/16h	8.5	95nm	1163	1038	21	26	60	19	36
1080°C/4h/70°C/min	760°C/16h	8.5	105nm	1147	989	30	31	49	22	42
1080°C/4h/30°C/min	760°C/16h	8.5	110nm - 310nm	1109	959	29	39	31	18	53

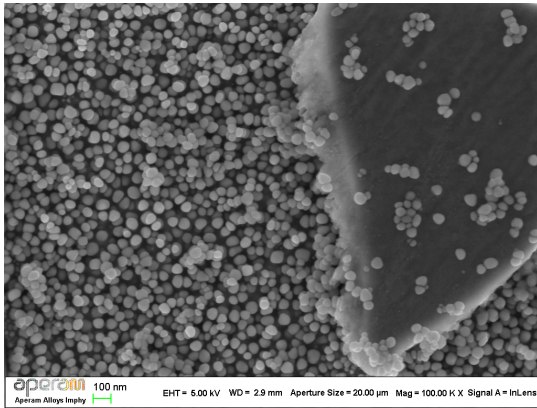
Table 4 : Effect of cooling rate after solution heat-treatment on mechanical properties and microstructure



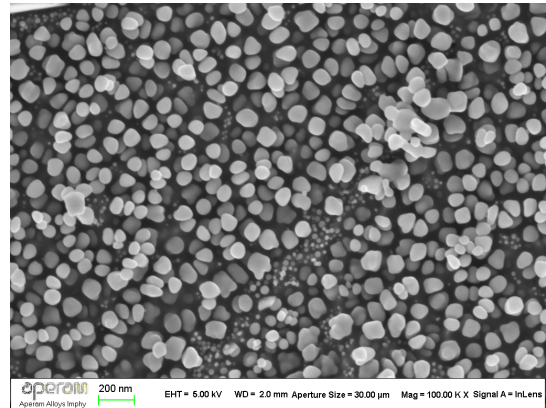
1060°C/4h/200°C/min + 760°C/16h/Air cooling



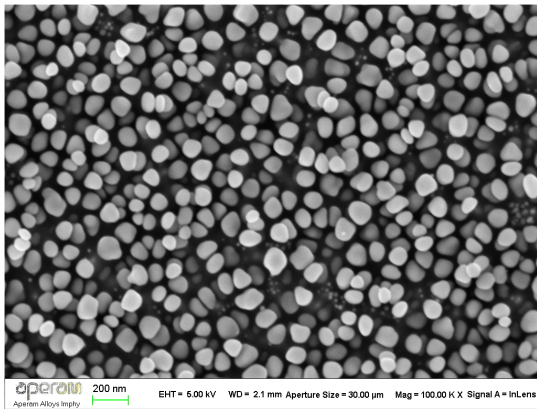
1120°C/4h/200°C/min + 760°C/16h/Air cooling



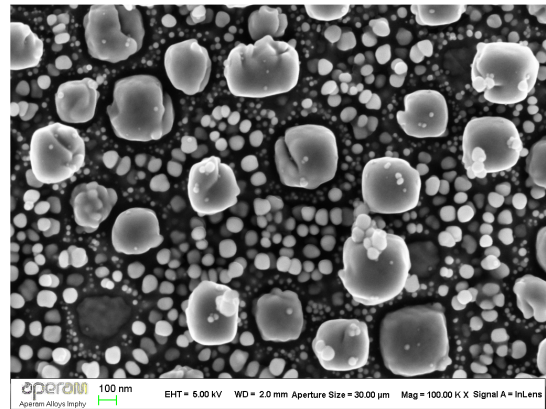
1080°C/4h/200°C/min + 760°C/16h/Air cooling



1080°C/4h/120°C/min + 760°C/16h/Air cooling



1080°C/4h/70°C/min + 760°C/16h/Air cooling



1080°C/4h/30°C/min + 760°C/16h/Air cooling

Figure 14 : SEM-FEG examinations made after various heat-treatments listed in tables 3 and 4

Coarser secondary  $\gamma'$  precipitates with a diameter close to 270nm are observed only after a solution heat treatment performed at 1060°C. It strongly suggests that these precipitates are fully dissolved above this temperature. These precipitates can not be rigorously considered as secondary  $\gamma'$  precipitates due to their presence before the cooling from solution heat treatment. A solution heat-treatment performed at 1060°C is not high enough to dissolve these secondary  $\gamma'$  precipitates formed during the previous cooling from the forging temperature. It is well established [13-15] that increasing cooling rate in  $\gamma/\gamma'$  superalloys leads to a decrease of the secondary  $\gamma'$  diameter. A bimodal precipitation of secondary  $\gamma'$  precipitates was observed for the lowest cooling rate and indicate that two precipitation waves occur during the cooling after solution heat treatment. As most of  $\gamma/\gamma'$  superalloys for turbine disks, mechanical properties of AD730™ are very sensitive to the solution heat-treatment temperature and strongly depend on  $\gamma'$  precipitates (secondary and tertiary) that have precipitated during the cooling after solution heat treatment (figure 15). The subsolvus solution heat-treatment was defined to obtain  $\gamma'$  dissolution as high as possible while controlling the grain size. Cooling rate after solution heat-treatment has to be as fast as possible to get the highest tensile and creep properties. Quenching can be easily performed on AD730™ without any issues due to the moderate gamma prime content in the alloy (37%) and the fine grain size. It is the reason why oil or polymer quenching after solution heat-treatment in the 1070-1080°C temperature range was preferred to perform mechanical tests on forged disks.

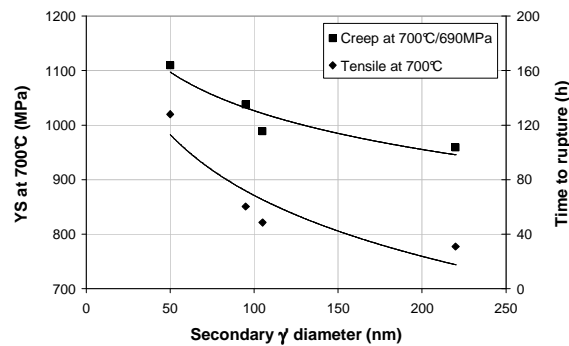


Figure 15 : Effect of secondary  $\gamma'$  precipitates diameter on the creep life and tensile yield strength

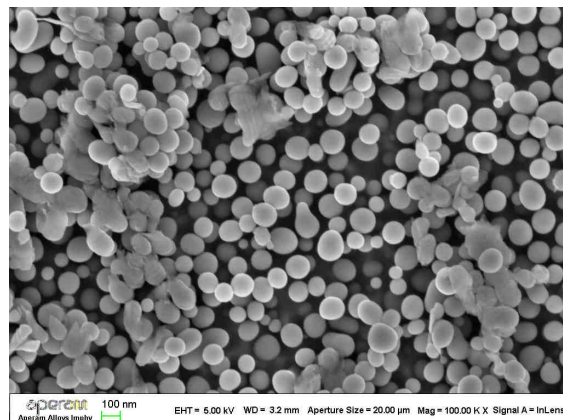
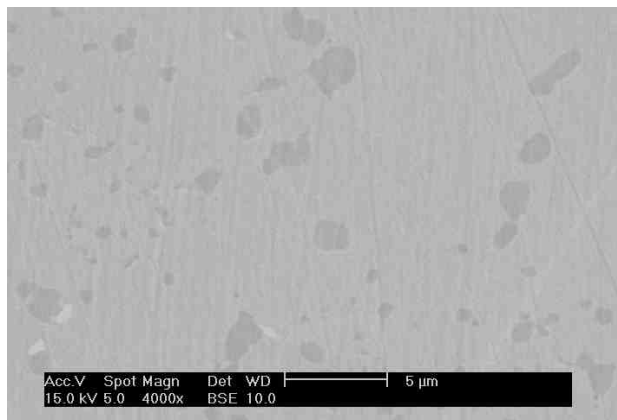


Figure 16: SEM-FEG examinations made after 1080°C/4h/200°C/min + 760°C/16h + 750°C/3000h

## Microstructural stability

AD730™ was designed to have a high microstructural stability by controlling Md parameter and TCP phases amount [1]. Microstructural stability was assessed on billet after a long-term aging of 3000h at 750°C which is very heavy compared to previous studies made on superalloys [16-18]. The initial heat-treatment before the long-term aging was 1080°C/4h/200°C/min + 760°C/16h. Various mechanical tests were performed before and after this long-term aging (table 5). As shown on figure 16, no TCP phases were observed on AD730™ after 3000h at 750°C. It explains that no embrittlement was observed after 3000h at 750°C with charpy notch impact tests and with tensile tests. This long-term aging leads to a slight increase of  $\gamma'$  secondary precipitates which explains the decrease of strength and creep life compared to the initial heat-treatment. This decrease of strength is reasonable (5-8%) and lower than those of other superalloys like 718Plus (13%), Waspaloy (14%) and U720Li (10-15%) in less severe conditions [17-19]. The size of secondary  $\gamma'$  precipitates was estimated to be close to 100nm after 3000h at 750°C (figure 16). It is interesting to notice that a similar  $\gamma'$  size and a similar creep life at 700°C-690MPa were obtained with a lower cooling rate equal to 70°C.min<sup>-1</sup> (table 4). The effect of long-term aging is therefore comparable to that of a slight decrease of cooling rate. It confirms that mechanical properties of AD730™ strongly depend on  $\gamma'$  precipitates size and that the microstructural stability of AD730™ is very high.

	1080°C/4h/200°C/min 760°C/16h	1080°C/4h/200°C/min 760°C/16h 750°C/3000h
Charpy notch impact (J)	31J	30J
Tensile 650°C	UTS	1368 MPa
	YS	1088 MPa
	El	28%
Creep 700°C 690MPa	tr	128 h
	El	10%
	RA	26%

Table 5: Mechanical properties after a long-term aging of 3000h at 750°C

### Mechanical properties on forged disk

Close-die forged disk of AD730<sup>TM</sup> was heat-treated with this following sequence: 1070°C/4h/Oil quenching + 760°C/16h/Air. As shown in table 6, a comparison was made with C&W superalloys for turbine disks in similar conditions: tests were performed on forged parts with similar grain size (in the ASTM 8-11 range) and similar cooling rate after solution heat-treatment.

	718	718Plus	U720Li	AD730 <sup>TM</sup>
SHT	975°C/1h	955°C/1h	1100°C/4h	1070°C/4h
Quenching	Oil	Oil	Oil	Oil
Aging	720°C/8h 620°C/8h	788°C/8h 704°C/8h	760°C/16h 650°C/24h	760°C/16h

Table 6 : Heat-treatment performed on forged disks of various C&W superalloys before mechanical tests

Tensile tests were performed from room temperature to 700°C. The tensile strength of AD730<sup>TM</sup> is significantly higher than those of 718 and 718Plus for the entire tested temperature range, and slightly higher than those of U720Li above 650°C. At 700°C, the yield strength of AD730<sup>TM</sup> is close to 1100MPa and 100MPa higher than that of 718Plus.

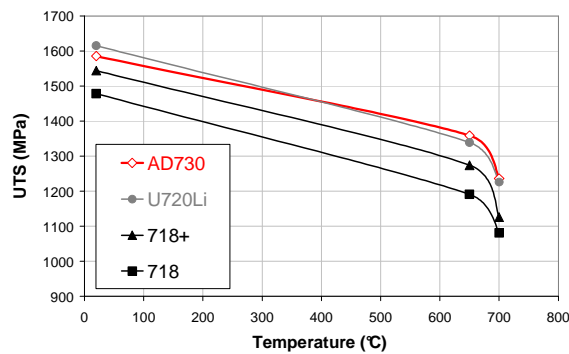


Figure 17: Ultimate tensile strength versus temperature for various C&W superalloys

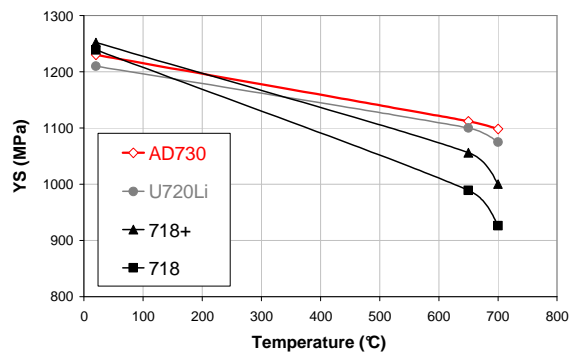


Figure 18: Yield strength versus temperature for various C&W superalloys

The density of AD730<sup>TM</sup> was measured to be equal to 8.2 g.cm<sup>-3</sup> and is in good agreement with previous results obtained on Ni30-Ni33 [2].

Stress-rupture properties were determined in temperatures ranging from 650°C to 760°C under various stresses. Time to rupture was analyzed using a Larson–Miller approach commonly employed for disk alloys (figure 19). As can be noted, AD730<sup>TM</sup> alloy exhibited great improvement in creep resistance compared to 718Plus and at least as good properties as those of U720Li. As the cost of AD730<sup>TM</sup> is lower than that of U720Li and similar to that of 718Plus, we can consider that the combination between cost and mechanical properties of AD730<sup>TM</sup> is higher than those of current C&W superalloys.

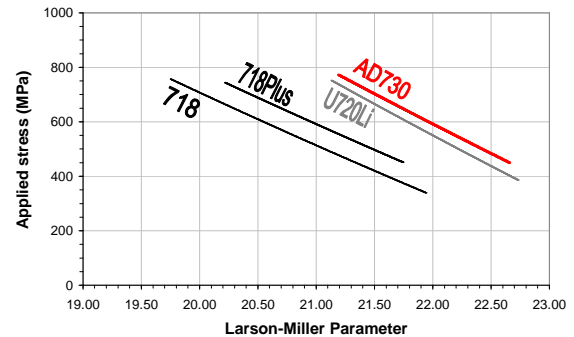


Figure 19: Creep properties of various C&W superalloys

### Conclusions

AD730<sup>TM</sup> was designed by Aubert & Duval to obtain similar properties to those obtained on previous work with Ni30 and Ni33. Only slight modifications were made on Ni30 and Ni33 chemistries to improve the workability and to avoid any risk of  $\eta$ -Eta phase precipitation. The presence of iron and the control of expensive elements provide to AD730<sup>TM</sup> a lower cost than other C&W superalloys. The workability of AD730<sup>TM</sup> was evaluated to be higher than those of Waspaloy and U720Li. Contrary to these C&W superalloys, AD730<sup>TM</sup> can be easily forged below and above  $\gamma'$  solvus. It is therefore possible to obtain a fine grain microstructure on the billet with a convenient forging process. Close-die forging discs and ring-rolling discs were forged without any issues and confirmed the good workability of AD730<sup>TM</sup>. As most of  $\gamma/\gamma'$  superalloys for turbine disks, mechanical properties of AD730<sup>TM</sup> are very sensitive to the solution heat-treatment and strongly depend on secondary and tertiary  $\gamma'$  precipitates. AD730<sup>TM</sup> presents a high microstructural stability. No TCP phases were observed after a long-term aging of 3000h at 750°C. This long-term aging leads to a slight increase of the secondary  $\gamma'$  precipitates and a slight decrease of the strength. Finally, tensile and creep properties of AD730<sup>TM</sup> are significantly higher than those of 718Plus and slightly higher than those of U720Li. Based on these results, the highest combination between cost and properties of AD730<sup>TM</sup> was therefore confirmed. Further work is going to be made to optimize the aging sequence in regard of tensile, creep and FCGR properties.

### Acknowledgment

Authors wish to thank the Imphy Research Center of APERAM for the quality of the SEM-FEG observations.



## References

- [1] A. Devaux, E. Georges, P. Héritier. "Development of new C&W superalloys for high temperature disk applications" Advanced Materials Research, Vol. 278 (2011) pp 405-410
- [2] A. Devaux, E. Georges, P. Héritier. "Properties of new C&W superalloys for high temperature disk applications". 7th International Symposium on Superalloy 718 and Derivatives, Edited by E.A. Ott et al., TMS 2010, pp 223-235
- [3] J.W. Brooks, P.J. Bridges. "Metallurgical stability of Inconel alloy 718". Superalloys 1988, Edited by S. Reichman et al., The Metallurgical Society 1988, pp 33-42
- [4] J.F. Barker. E.W. Ross. J.F. Radavich. "Long time stability of Inconel 718". Journal of metals, January 1970, pp 31-41.
- [5] A. Devaux. L. Nazé. R. Molins. A. Pineau. "Gamma double prime precipitation kinetic in alloy 718". Materials Science and Engineering A 486 (2008) pp 117-122
- [6] C.Y. Cui. Y.F. Gu. H. Harada. D.H. Ping. A. Sato. "Phase stability and yield stress of Ni-base superalloys containing High Co and Ti". Metallurgical and Materials Transactions, Vol 37A, November 2006, pp 3183-3190
- [7] C.Y. Cui. Y.F. Gu. H. Harada. A. Sato. "Microstructure and yield strength of Udimet 720Li alloyed with Co-16.9 Wt Pct Ti". Metallurgical and Materials Transactions, Vol 36A, November 2005, pp 2921-2927
- [8] Y.F. Gu. C. Cui. H. Harada. D.H. Ping. "Development of Ni-Co base alloys for high-temperature disk applications", Superalloys 2008, Edited by R.C. Reed et al., TMS 2008, pp 53-61
- [9] R.L. Kennedy. "Allvac 718Plus, superalloy for the next forty years". Superalloys 718. 625. 706 and derivatives, TMS 2005, pp 1-14.
- [10] W.-D. Cao. R.L. Kennedy. "Role of chemistry in 718-type alloys allvac 718plus alloy development". Superalloys 2004, Edited by K.A. Green et al, TMS 2004, pp 91-100
- [11] Paul D. Jablonski. Christopher J. Cowen. and Jeffery A. Hawk. "Effects of Al and Ti on Haynes 282 with fixed gamma prime content". 7th International Symposium on Superalloy 718 and Derivatives. Edited by E.A. Ott et al., TMS 2010, pp 617-628
- [12] JR. Vaunois, J. Cormier, P. Villechaise, A. Devaux, B. Flageolet. "Influence of both  $\gamma'$  distribution and grain size on the tensile properties of UDIMET 720Li at room temperature". 7th International Symposium on Superalloy 718 and Derivatives, Edited by E.A. Ott et al, TMS 2010, pp 199-213
- [13] R. Radis, M. Schaffer, M. Albu, G. Kothleitner, P. Pölt, E. Kozeschnik. "Evolution of size and morphology of  $\gamma'$  precipitates in Udimet 720Li during continuous cooling". Superalloys 2008, Edited by R.C. Reed et al, TMS 2008, pp 829-836
- [14] J. Mao, K. Chang, Y. Wanhong, K. Ray, S. Vaze, D. Furrer. "Cooling precipitation and strengthening study in powder metallurgy superalloy U720Li", Metallurgical and materials transactions A, Vol 32A, October 2001, pp 2441-2452
- [15] J. Tiley, G.B. Viswanathan, R. Srinivasan, R. Banerjee, D.M. Dimiduk, H.L. Fraser. "Coarsening kinetics of  $\gamma'$  precipitates in the commercial nickel base Superalloy René 88 DT", Acta Materialia, Volume 57, Issue 8, May 2009, pp 2538-2549
- [16] Wei-Di Cao, "Thermal stability characterization of Ni-base ATI 718Plus superalloy", Superalloys 2008, Edited by R.C. Reed et al, TMS 2008, pp 789-797
- [17] D. Helm and O. Roder, "Influence of Long Term Exposure in Air on Microstructure, Surface Stability and Mechanical Properties of UDIMET 720LI," Superalloys 2000, ed. T.M. Pollock et al., TMS 2000, pp. 487-493.
- [18] S. Mannan, S. Patel, J. De Barbadillo. "Long Term Stability of INCONEL Alloys 718, 706, 909, and Waspaloy at 593C and 704C," Superalloys 2000, ed. T.M. Pollock et al., TMS 2000, pp. 449-458